



GEO Québec  
2015

Challenges from North to South  
Des défis du Nord au Sud

# Numerical study for soil-spring stiffness of pile group

L. Hazzar<sup>(a)</sup>, M. Karray<sup>(a)</sup> & A. Pasic<sup>(b)</sup>

<sup>(a)</sup>Department of Civil Engineering, University of Sherbrooke, Sherbrooke,  
Québec, Canada

<sup>(b)</sup>Dessau Inc. - Bridge and Structures, Québec, Québec, Canada

## ABSTRACT

Many approaches have been developed to determine the soil-spring stiffness and typical values have been proposed for different types and densities of soil. However, these typical values ignore the effect of the depth and the degradation of elastic parameter (G or E) as a function of strain. In this paper, a series of 3D numerical analyses are conducted to compute the equivalent soil-spring stiffness's according to pile distortion for a pile group located under the central pier of bridge structure above the river Sault-au-Mouton (Longue-Rive, Quebec) and subjected to multi-loading conditions. In these simulations the degradation of the shear modulus is incorporated in order to account for soil nonlinearity. The idea is to develop equivalent springs that can be adapted to the lateral deformation of the pile. The stiffness of these springs thus varies depending on the distortion and may be adapted in an iterative process according to the pile deformation at each depth. This method can be compared to the linear equivalent method used in dynamic analysis where an equivalent shear modulus is adapted according to the shear distortion. In fact, This type of linear equivalent spring is very useful for structural engineers who want to incorporate the effect lateral capacity of soil in their models.

## RÉSUMÉ

Des nombreuses approches ont été développées pour déterminer la rigidité du sol-ressort et des valeurs typiques ont été proposées pour différents types et densités du sol. Toutefois, ces valeurs typiques ne tiennent pas compte de l'effet de la profondeur et de la dégradation de paramètre élastique (G ou E) en fonction de la déformation. Dans cet article, une série d'analyse numériques 3D ont été réalisées pour déterminer les rigidités équivalentes des ressorts dans le sol en fonction de la distortion du pieu pour un groupe de pieux situé sous le pilier central de la structure d'un pont au-dessus de la rivière Sault-au-Mouton (Longue-Rive) et soumis à plusieurs chargements. La dégradation du module de cisaillement est prise en compte afin de tenir compte de la non-linéarité du sol. L'idée est de développer des ressorts équivalents qui peuvent être adaptés à la déformation latérale du pieu. Les rigidités de ces ressorts varient en fonction de la distortion et peuvent être adaptés dans un processus itératif selon la déformation du pieu à chaque profondeur. Cette méthode peut être comparée à la méthode linéaire équivalente utilisée dans l'analyse dynamique où un module de cisaillement équivalent est calculé en fonction de la déformation de cisaillement. En réalité, Ce type de ressort équivalent linéaire est très utile pour les ingénieurs en structure qui veulent intégrer l'effet de la capacité latérale du sol dans leur modèles.

## 1 INTRODUCTION

The behavior of laterally loaded piles is a complex soil structure interaction problem that has received a considerable amount of attention over the last four decades mainly in the field of offshore engineering or earthquake geotechnical engineering due to large stakes involved. The primary function of a pile or a group of piles is to transfer the external loads from the superstructure to the surrounding soil medium without causing excessive deflections at the top of the pile or piles. The analysis of such a problem is complicated because of the complex stress-strain behavior of the soil surrounding the piles. In practice, analysis of laterally loaded piles is carried out using beams on non-linear Winkler springs model (often known as p-y method) due to its simplicity, low computational cost and the ability to model layered soils. In this approach, soil-pile interaction along the depth is characterized by a set of discrete non-linear springs represented by p-y curves where  $p$  is the pressure on the soil that causes a relative pile deformation of  $y$ . A number of different methods are in use to construct the p-y curves (Matlock, 1970; Cox et al., 1974; Reese et al., 1974; Reese et Van Impe, 2001) usually constructed based on semi-empirical correlations. Subsequently, many

approaches (Terzaghi, 1955; Vesic, 1961; Broms 1964a, 1964b; Ménard et al., 1969; Davisson 1970; Matlock, 1970; Poulos, 1971; Gilbert 1995) have been developed to determine the soil-spring stiffness and typical values has been proposed for different type of soils and for different densities. However, these typical values generally ignore the effect of depth and the degradation of elastic parameter of the (G or E) as a function of strain.

In Québec, Broms's method is still used in the current design practice of piles under lateral loads (CGS, 2013). This empirical method is not entirely appropriate for the design of complex structure such as bridge, which needs sophisticated three dimensional (3D) numerical analysis. In this 3D modeling, the soil behavior should be simulated by a series of springs that surround the pile foundation. Thus, several questions were asked by the engineers (essentially structural engineers):

- What are the appropriate values of the horizontal stiffness of the springs in the soil around the piles?
- What are the values of the stiffness of the soil during seismic loading?
- What are the group reduction factors that must apply to reflect the pile group effects?

In view of the above stated issues and to answer these previous questions, this paper describes and

discusses the results of a series of 3D finite difference FD analyses using the program *FLAC<sup>3D</sup>* (Itasca 2009). The 3D numerical analyses are carried out to investigate the soil-spring stiffness of pile group located under the central pier of bridge structure above the river Sault-au-Mouton (Longue-Rive, Quebec) and subjected to multi-loading conditions (vertical load, lateral loads and moments).

## 2 COEFFICIENT OF SUBGRADE REACTION

The Winkler method, or sometimes known as the subgrade reaction method, currently appears to be the most widely used in a design of laterally loaded piles. The method was first introduced by Winkler (1867) to analyze the response of beams on an elastic subgrade by characterizing the soil as a series of independent linearly-elastic soil springs. Since then, this concept has been extensively employed for the laterally loaded pile problem. The concept of this method is graphically illustrated in Figure 1.

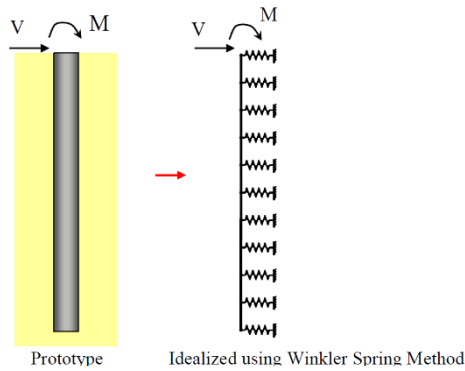


Figure 1. Implementation of Winkler spring concept for laterally loaded pile problem.

The term of subgrade reaction indicates the lateral pressure,  $p$ , per unit area of the surface of the contact between a loaded beam or slab and the subgrade on which it rests and on to which it transfers the loads. The coefficient of subgrade reaction,  $k$ , is the ratio between the soil lateral pressure,  $p$ , at any given point of the surface of contact and the lateral deflection,  $y$ , produced by the load application at that point:

$$k = \frac{p}{y} \quad [1]$$

The soil-spring stiffness or the modulus of subgrade reaction,  $E_s$  ( $\text{kN/m}^2$ ) is related to the pile diameter,  $B$  by the following equation:

$$E_s = k \cdot B \quad [2]$$

Though simple in its definition, the modulus of subgrade reaction has proved to be a very difficult parameter to evaluate. This is because it cannot be measured in laboratory tests, but must be back-calculated from full-scale field tests. Investigations have shown it to

be variable not only with the soil type and mechanical properties, but also with stress level and the geometry of the pile. In the absence of better information, the coefficient of horizontal subgrade reaction may be estimated by several methods (Hazzar, 2014).

It is evident that the Winkler model (Fig. 2) cannot fully capture the 3D aspect of soils. The fundamental assumption on which the technique of constructing a  $p$ - $y$  curve is based is the similarity between the load deformation pattern of pile head and the stress-strain behaviour of the interacting soil from carefully chosen element testing (e.g., triaxial tests).

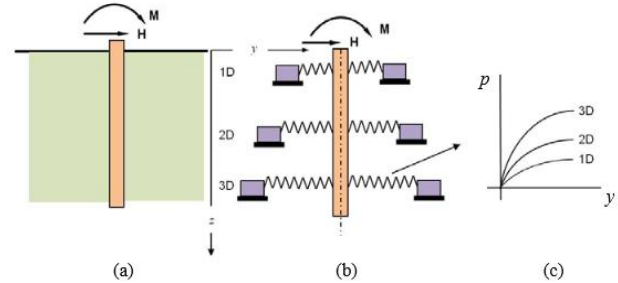


Figure 2. Single pile under lateral loading: (a) real vertical pile; (b) Winkler idealization; (c)  $p$ - $y$  curves for lateral Winkler springs.

## 3 GROUP PILES UNDER MULTI-LOADS

### 3.1 Description of the bridge project

The project consists of a bridge structure above the river Sault-au-Mouton (Longue-Rive, Quebec). Figure 3 shows the location of the study site.

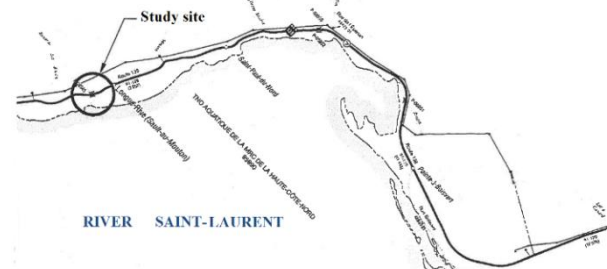


Figure 3. Site location.

The bridge deck contains two spans, each 75 m in length and 14.0 m in width. According to the architectural plan of the bridge, the footings will be positioned at elevations following:

- West Abutment: top of the footing directly below the ground surface at the elevation of 37.78 m;
- Central pier: above the sole directly under the surface of the riverbed elevation at 27.265 m;
- Abutment: above the sole to 38.495 m elevation in the approach embankment.

The central pier is supported by a footing that is supported by a group of 6 drilled shaft piles (figure 4).

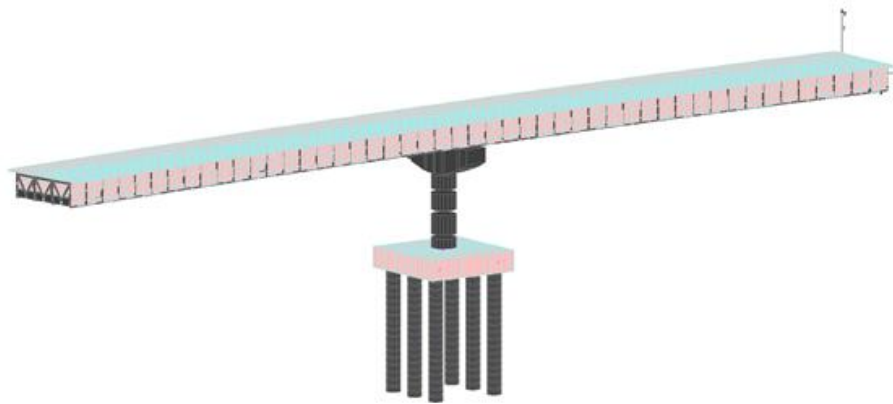


Figure 4. Bridge P-15705 in Longue-Rive, 3D modeling.

### 3.2 Soil properties

A total of eight boreholes, identified F25 to F32, were made in 2004 to investigate the soil conditions and to determine the roc position. The soil profile is constituted by two sandy layers with groundwater at the surface. Table 1 summarizes the properties of these soil layers.

Table 1. Soil properties after geotechnical tests

Depth (m)	0.0-6.0	6.0-20.0
Unit weight, $\rho_w$ (kN/m <sup>3</sup> )	21.00	21.00
Angle of friction, $\phi$ (°)	35.00	40.00
Shear velocity, $V_s$ (m/s)	200.00	230.00
Poisson' ratio, $\mu$	0.33	0.33

### 3.3 Piles properties

A total of 6 drilled shaft piles are installed. The piles have a diameter  $B$  of 2.0 m and a length  $L$  of 16 m. Configuration of  $2 \times 3$  piles has been proposed with spacing of 5.0 m  $\times$  10.0 m. the mechanical characteristics of the pile are: a Poisson's ratio  $\mu_p$  of 0.20 and a modulus of elasticity  $E_p$  of 25 GPa.

### 3.4 Types of loads applied to the bridge

The bridge is located in seismic performance zone 3. Referring to the specification of the CAN/CSA-S6-06 (2006) code, this structure is classified in the category of lifeline bridge. Subsequently, a seismic analysis with multi-mode spectral method is considered and 3 loading cases have been analyzed (Table 2):

- Case n°1: applied forces without taking into account the seismic excitation;
- Case n°2: applied forces taking into account a 100% transversal seismic excitation and a 30% longitudinal seismic excitation ;
- Case n°3: applied forces taking into account the 100% longitudinal seismic excitation and the 30% transversal seismic excitation;

Table 2. Values of applied forces.

Case n°	1	2	3
Lateral load, $P_x$ (kN)	123	2.280	7.010
Axial load, $P_y$ (kN)	39.152	28.100	27.800
Lateral load (kN)	1.950	3.150	1.340
Bending moment, $M_x$ (kN.m)	30.000	53.010	22.200
Torque, $M_y$ (MN.m)	1.800	120	350
Bending moment, $M_z$ (kN.m)	1.900	37.100	113.500

## 4 FINITE DIFFERENCES MODELLING

### 4.1 Finite differences mesh and boundary conditions

The 3D FD program *FLAC<sup>3D</sup>* (Itasca, 2009) was employed to study the behavior of a single pile and pile groups (lateral displacement, lateral resistance and stiffness of each pile) under several loads. Figures 5 and 6 show 3D finite difference grids used in the numerical analyses.

A mesh generator subroutine was implemented using the *FISH* built-in programming language providing the possibility of mesh refinement and geometry variation. The bottom elevation and the lateral sides of the computational domain were taken far enough from the group to avoid any significant boundary effect. Based on the experience gained through this and previous numerical works, a mesh refinement around the piles leads to a more accurate distribution of stresses and soil yielding. In order to make sure that the zones size has no effect on the response of the characteristic piles, trial analyses have been carried out to optimise mesh discretization. More specifically, the response of each characteristic pile has been established carrying out an analysis in which only this pile was activated. The responses of these piles have then been compared and re-adjustment of the mesh was done if necessary.

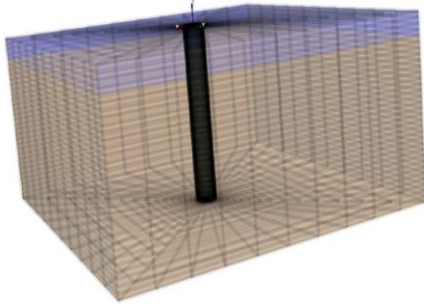


Figure 5. Three dimensional single pile model.

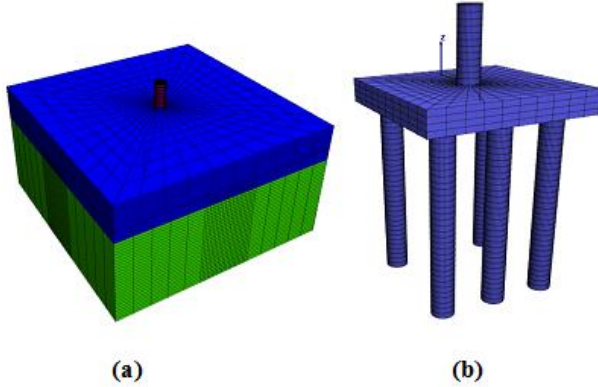


Figure 6. Finite differences mesh for a 5x3 pile group: (a) Global model and (b) pile group with footing.

#### 4.2 Soil model

The Mohr-Coulomb's law (M.C.) constitutive relation was used to model soil layers. In fact, it allows us to define shear failure of a soil mass based on its state of stress. This elastic perfectly-plastic model requires five basic input parameters, namely a maximum elastic bulk modulus " $K_{max}$ ", maximum elastic shear modulus " $G_{max}$ ", mass density " $\rho$ ", undrained shear strength " $c_u$ " and the friction angle " $\phi$ ".

For sandy soils,  $G_{max}$ , is estimated from the shear wave velocity,  $V_s$ , and the mass density,  $\rho$ , by the correlation:

$$G_{max} = \rho V_s^2 \quad [2]$$

The maximum elastic bulk modulus,  $K_{max}$  is related to  $G_{max}$  and the Poisson's ratio,  $\mu$  by:

$$K_{max} = G_{max} \frac{2(1+\mu)}{(3-6\mu)} \quad [3]$$

Therefore, the material properties adopted in the analyses for the two layers (referred to the properties deduced from geotechnical tests) are presented in Table 3.

Table 3. Soil parameters according to M.C.

Depth (m)	$\rho$ (kg/m <sup>3</sup> )	$G_{max}$ (MPa)	$K_{max}$ (MPa)	$c_u$ (kPa)	$\phi$
0.0-6.0	2100	5.40	11.70	0	35
6.0-20.0	2100	12.60	27.30	0	40

Standard elastic/plastic constitutive laws such as Mohr-Coulomb (M.C.) can also produce the reduction of shear-modulus that can be evaluated from degradation curves as follows: consider the M.C. model with a constant shear modulus,  $G_{max}$ , and a constant yield stress,  $\tau_m$ , corresponding to cyclic shear strain of amplitude,  $\gamma$ . In pre failure phase, the secant shear modulus,  $G$ , is assumed to be equal to  $G_{max}$ . For a cyclic excitation that involves failure, the secant modulus is given by:

$$G = \frac{\tau_m}{\gamma} \quad [4]$$

The shear modulus-reduction curve relates the ratio  $G/G_{max}$  to the amplitude of shear strain,  $\gamma$ ; it is simply obtained from Eq. 5 by setting  $\gamma_m = \tau_m / G_{max}$ , one obtains, for  $\gamma > \gamma_m$ ,

$$\frac{G}{G_{max}} = \frac{\gamma_m}{\gamma} \quad [5]$$

For numerical simulation, the recognised shear-modulus degradation curve proposed by Seed and Idriss (1970) for sands soils is adopted (Figure 7).

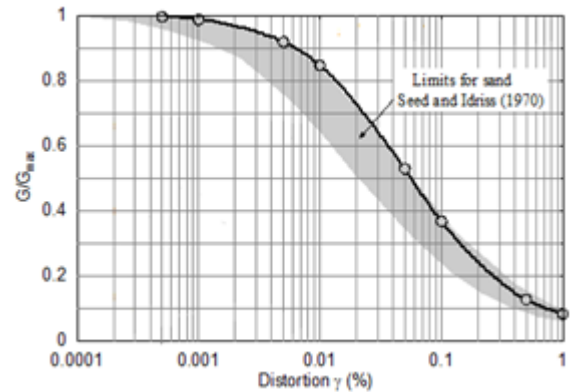


Figure 7. Adopted curve of shear modulus degradation for sandy soils (Seed and Idriss, 1970).

#### 4.3 Pile model

The pile is modelled as linear-elastic material. Three parameters are required to define the pile material behavior. These parameters are the elastic bulk modulus,  $K_p$ , the elastic shear modulus,  $G_p$ , and the mass density,  $\rho_p$ .

#### 4.4 Soil-pile interface model

The interface elements are modeled by the linear Coulomb shear-strength criterion that limits the shear force acting at an interface node. The shear-strength criterion that limits the shear force acting at an interface node for sandy soils is given by Eq. (6).

$$F_{s\max} = (F_n - p_1 A) \tan \phi_i \quad [6]$$

Where  $F_{s\max}$  is the limiting shear force at pile-soil interface,  $F_n$  is the normal force,  $\phi_i$  is the angle of friction of the interface surface,  $p_1$  is pore pressure (interpolated from the target face) and  $A$  is the contact area between pile and soil.

The value of friction angle of the interface surface corresponds to critical state and is reduced compared to the friction angle of the surrounding soil (Ortigao, 1995). Separation is able to cause a significant increase in displacements (Poulos and Davis, 1980) and therefore the interface elements are allowed to separate if tension develops across the interface and exceeds the tension limit of the interface. Once gap is formed between the pile-soil interfaces, the shear and normal forces are set to zero.

The normal and shear forces at the interface nodes are determined by the following equations:

$$F_n^{(t+\Delta t)} = k_n u_n A + \sigma_n A \quad [7]$$

$$F_{si}^{(t+\Delta t)} = F_{si}^{(t)} + k_s \Delta u_{si}^{(t+0.5\Delta t)} + \sigma_{si} A \quad [8]$$

Where  $F_n$  and  $F_{si}$  are the normal and shear force, respectively,  $k_n$  and  $k_s$  the normal and shear stiffness, respectively,  $\Delta u_{si}$  the incremental relative shear displacement vector,  $u_n$  the absolute normal penetration of the interface node into the target face,  $\sigma_n$  the additional normal stress added due to interface stress initialization, and  $\sigma_{si}$  the additional shear stress vector due to interface stress initialization.

In many cases, particularly when linear elastic analysis is performed, values for interface stiffness are assigned to simulate the nonlinear behavior of a physical system. In the present study, where nonlinear analysis is carried out, the value for the interface stiffness should be high enough, in comparison with the surrounding soil, in order to minimize the contribution of those elements to the accumulated displacements. According to the results of numerical analyses a value of  $10^9$  MPa/m for both  $k_n$  and  $k_s$  was sufficient to ensure that no additional deflections were attributed to the pile due to the deformation of the springs representing the interface. The use of considerably higher values is tempting as it could be considered as more appropriate, but in that case the solution convergence would be very slow.

#### 4.5 Lateral deflection of pile

When a pile is laterally loaded, the nodes move along the direction of applied load in large strain mode. Therefore, it is not possible to identify a particular node after loading using its original coordinate. To calculate the lateral

deflection of the pile,  $y$ , first the coordinates of all the nodes of the vertical pile axis were stored in the memory of the computer. Once the model reached equilibrium, the same nodes were identified and their displacements calculated by subtracting their initial and final horizontal coordinate.

#### 4.6 Soil lateral pressure

The soil lateral pressure,  $p$ , can also be calculated by summing the forces in the relevant direction acting on the soil-pile interface nodes at the same depth. A schematic of the pile-soil system is presented in Fig. 8. Each interface node is associated with a normal force and a shear force (Hazzar, 2014).

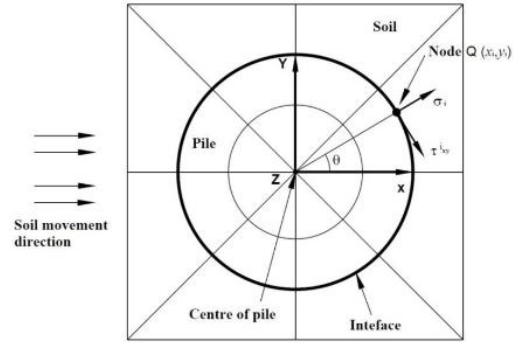


Figure 8. Schematic plot of pile-soil system with interface between them (Hazzar, 2014).

The x-component of the lateral pile-soil pressure is summed over all the interface nodes to calculate the lateral soil pressure,  $p$  per unit length along the pile at a particular pile section and is expressed as:

$$p = \sum_{i=1}^n ((\sigma_i n_{x,i} + \tau_{xy,i} n_{y,i}) \times A_i) \quad [9]$$

Where,

$$n_{x,i} = \cos \theta = \frac{x_i}{\sqrt{x_i^2 + y_i^2}}$$

$$n_{y,i} = \sin \theta = \frac{y_i}{\sqrt{x_i^2 + y_i^2}}$$

$\sigma_i$  : normal stress at the interface node at point Q;

$\tau_{xy,i}$  : shear stress at the interface node at point Q;

$x_i$  : x-coordinate of the interface node at point Q;

$y_i$  : y-coordinate of the interface node at point Q;

$A_i$  : representative area of interface node.

## 5 NUMERICAL RESULTS AND DISCUSSIONS

Based on the constitutive model parameters described previously, the response of the laterally loaded single pile is presented in terms of p-y curves stiffness of equivalent soil-spring versus pile distortion. For group piles, the response is presented in terms of pile group effects.

## 5.1 Stiffness of equivalent soil-spring

The most widely used nonlinear analysis for laterally loaded piles is the p-y curves. In this paper p-y curves are obtained based the methods of prediction of lateral deflection,  $y$  and lateral pressure,  $p$ , described in sections 4.5 and 4.6 respectively.

Figure 9 shows numerical p-y at seven depths of the pile. It is clear that the lateral pressure of soil increases as the depth does. This can be explained by a decrease in lateral deflection with depth.

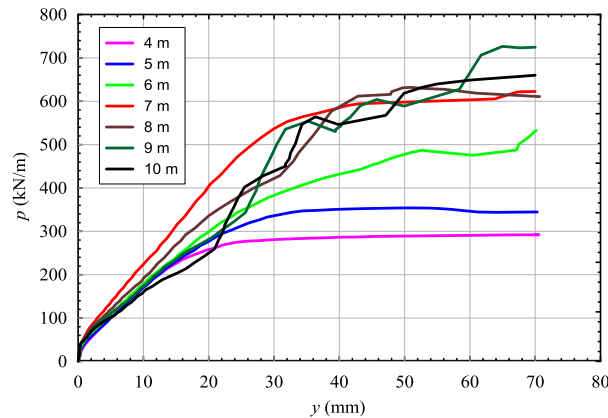


Figure 9. p-y curves between 4 and 10 m of depth.

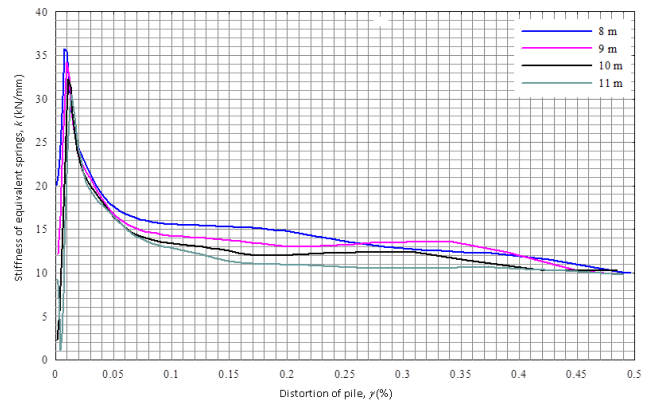
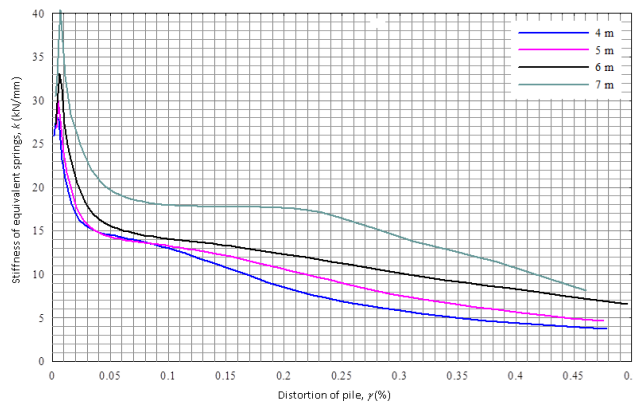


Figure 10. Stiffness of equivalent spring-soil versus distortion of pile between 4 and 11 m of depth.

Table 4. Modulus of subgrade reaction,  $E_s$  (kN/mm): Comparisons between the current analysis and several methods.

Depth (m)	Current analysis	Broms (1964b)	Ménard et al. (1969)	Poulos (1971)	Gilbert (1995)
0.0-6.0	4 to 33	22.0	25.0	11.8	26.96
6.0-20.0	2 to 40	22.0	32.0	27.5	30.9

## 6 CONCLUSIONS

For prediction the spring-soil stiffness of piles group under multi-loads (lateral load, axial load and torque), a series of rigorous 3D numerical analysis based on finite difference technique has been performed. The Mohr Coulomb criterion is used to model the soil parameters and recognised shear-modulus degradation curve given by

Seed and Idriss (1970) to adjust the value of shear modulus of soil is considered. According to the definition of modulus of subgrade reaction or spring-soil stiffness in section 2, the variation of the stiffness of equivalent springs, with the distortion of pile are plotted for at several depths in Fig. 10. Figure 10 indicates that the stiffness's of spring-soils are not constants as they have already mentioned the most methods considered in practice (Hazzar, 2014). Table 4 shows the spring-soil stiffness predicted by the current numerical analysis and those given by several methods adopted in the practice. According to Table 4, these methods give reasonable values but ignore the effect of depth and the pile distortion.

## 5.2 Piles group effects

The lateral response (profiles of lateral deflection and lateral pressure) of the pile group 2x3 are studied with  $FLAC^{3D}$  for the several loads conditions (Table 3). The results are compared with the lateral response of single pile. Consequently group reduction factors are determined for the equivalent spring-soil stiffness along the depth (Table 4). It can be seen that these reduction factors increase with depth and its values depend of the location of each pile in the group.

Seed and Idriss (1970) to adjust the value of shear modulus of soil is considered.

The results obtained are interpreted rationally to conclude, initially, that the stiffness's of equivalent springs vary depending on the pile distortion and may be adapted in an iterative process according to the pile deformation at each depth. This process can be compared to the linear equivalent method used in dynamic analysis where an equivalent shear modulus is adapted according to the

shear distortion. This type of linear equivalent spring is very useful for structural engineers who want to incorporate the effect of lateral capacity of soil in their model. Secondly, the reduction factors to reflect the group effects depends of the depth and the location of each pile in the group (consequently the spacing between the piles).

Table 4. Factors of reduction to reflect the group effects.

Depth (m)	Factor of reduction / longitudinal direction	Factor of reduction / transversal direction / middle piles	Factor of reduction / transversal direction / back piles
4	0.49	0.13	0.45
5	0.48	0.14	0.38
6	0.51	0.10	0.39
7	0.51	0.09	0.42
8	0.52	0.12	0.49
9	0.53	0.21	0.62
10	0.53	0.34	0.70
11	0.53	0.51	0.90
12	0.58	0.73	1
13	0.72	0.95	1
14	0.88	>1	>1
15	>1	>1	>1
16	>1	>1	>1
17	>1	>1	>1
18	>1	>1	>1
19	>1	>1	>1

## REFERENCES

- Broms, B.B. 1964a. Lateral resistance of piles in cohesive soils, *Journal of Soil Mechanics. Foundation Division, ASCE*. 90(2): 27-64.
- Broms, B.B. 1964b. Lateral resistance of piles in cohesionless soils, *Journal of Soil Mechanics. Foundation Division, ASCE*. 90(SM3): 123-156.
- Cox, W. R., Reese, L.C., Grubbs B.R. 1974. Field testing of laterally loaded piles in sand, *Proceedings of the 6<sup>th</sup> Annual Offshore Technology Conference, Houston, Texas*. OTC 2079, 14 pages.
- CAN/CSA-S6-06. 2006. Canadian Highway Bridge Design Code, CSA group, 930 pages.
- CGS. 2013. Canadian Foundation Engineering Manual (4<sup>th</sup>Ed.), Richmond, B.C., Canadian Geotechnical Society.
- Davisson, M.T. 1970. Lateral load capacity of piles, *Highway Research. Record* 333: 104-112.
- Hazzar, L. 2014. Analyse numérique de la réponse des pieux sous sollicitations latérales, PhD. Université de Sherbrooke (Québec-Canada), 214 pages.
- Itasca Consulting Group. 2009. *FLAC3D: Fast lagrangian analysis of continua in 3-dimensions 4.1, manual*. Itasca, Minneapolis.
- Gilbert, C. 1995. Une nouvelle approche des calculs d'interaction sol-structure, *Révue Française de Géotechnique*. 7: 3-9.
- Ménard, L., Bourdon, G., Gambin, M. 1969. Méthode générale de calcul d'un rideau ou d'un pieu sollicité latéralement en fonction des résultats pressiométriques, *Sols-Soils*, 22-23: 16-29.
- Matlock, H. 1970. Correlations for design of laterally loaded piles in soft clay. *Journal Soil Mechanics and Foundations, ASCE*. SM5: 63-91.
- Ortigao, J.A. 1995. Soil mechanics in the light of critical state theories. Rotterdam: Balkema.
- Poulos, H.G. 1971. Behaviour of laterally loaded piles: I-single piles. *Journal Soil Mechanics and Foundation, ASCE*. 5(97): 711-31.
- Poulos, H.G., Davis, E.H. 1980. *Pile foundation analysis and design*. New York: John Wiley & Sons Ltd.
- Reese, L. C., Cox, W.R., Kooper, F.D. 1974. Analysis of laterally loaded piles in sands. *Proceedings of the 6<sup>th</sup> Annual Offshore Technology Conference, Houston, Texas*. OTC 2080: 437-483.
- Reese, L.C., Van Impe, W.F. 2001. Single piles and pile groups under lateral loading. A.A. Balkema, Rotterdam. 508 pages.
- Seed, H.B., Idriss, I.M. 1970. Soil moduli and damping factor for dynamic response analyses. Report No. EERC 70-10, Earthquake Engineering Research Center, University of California, Brekeley, California.
- Terzaghi, K. 1955. Evaluation of coefficients of subgrade reaction. *Géotechnique*. 5: 297-326.
- Vesic, A. 1961. Design of pile foundations. National cooperative highway research program synthesis of highway practice. Report No. 42, Transportation Research Board, Washington, D.C., 68 pages.
- Winkler, E. 1867. Die lehre von der elasticita et und festigkeit. Prag, Dominicus